

# Methods

This section gives an overview of the methods used to obtain the four shear wave velocity data sets presented in the CD-ROM.

Seismic cone penetrometer

Borehole Shear Wave Velocity Logs

Surface Shear Wave Refraction Soundings

Seismic lines (Dynamic Oil) with  
shear wave velocity analysis locations

Borehole Geophysics

Menu

Continue

Quit

## SEISMIC CONE PENETROMETER MEASUREMENTS

Shear wave velocities were measured using an 8 hz horizontal geophone installed behind the tip of a conventional cone penetrometer (see figure 1) designed and operated by CONETEC Investigations Ltd. of Vancouver, B.C. The cone is a 10 ton compression design with a standard tip area of 10 sq. cm. and a friction sleeve aread of 150 sq. cm. The cone was pushed using a modified drilling rig (MARL-10) with a maximum thrust of 14 tons, operated by Mud Bay Drilling Co. Of Surrey, B.C. The cone bearing, sleeve friction and dynamic penetrometer pore pressure results from SCPT sites are reported elsewhere (Woeller et al., 1994; Christian et al., 1994; Woeller et al., 1993a, Woeller et al., 1993b, Hunter et al., 1991;, Robertson et al., 1990; Finn et al., 1989a; Finn et al., 1989b).

Shear wave velocities were measured at 1 meter intervals during cone pushes (i.e. when the cone rods were disconnected from the drilling rig). The source was a 7.5 kgm hammer striking a horizontal plate (under load from the drilling rig); the source was generally 1 to 2 meters offset on surface to the cone hole. Two polarized source directions were recorded for each subsurface location using a digital stacking oscilloscope. Onset of shear wave motion at the geophone was interpreted using standard reversing-polarity techniques (Robertson et al. 1986).

An example of a composite depth plot of geophone traces (one polarity only) is shown in Figure 2.

Shear wave travel times between each successive geophone location were used to compute the interval shear wave velocity between locations; straight line travel path source-offset corrections were made. The calculated shear wave velocities are plotted at the mid-point between geophone locations on the velocity-depth plots for all sites.

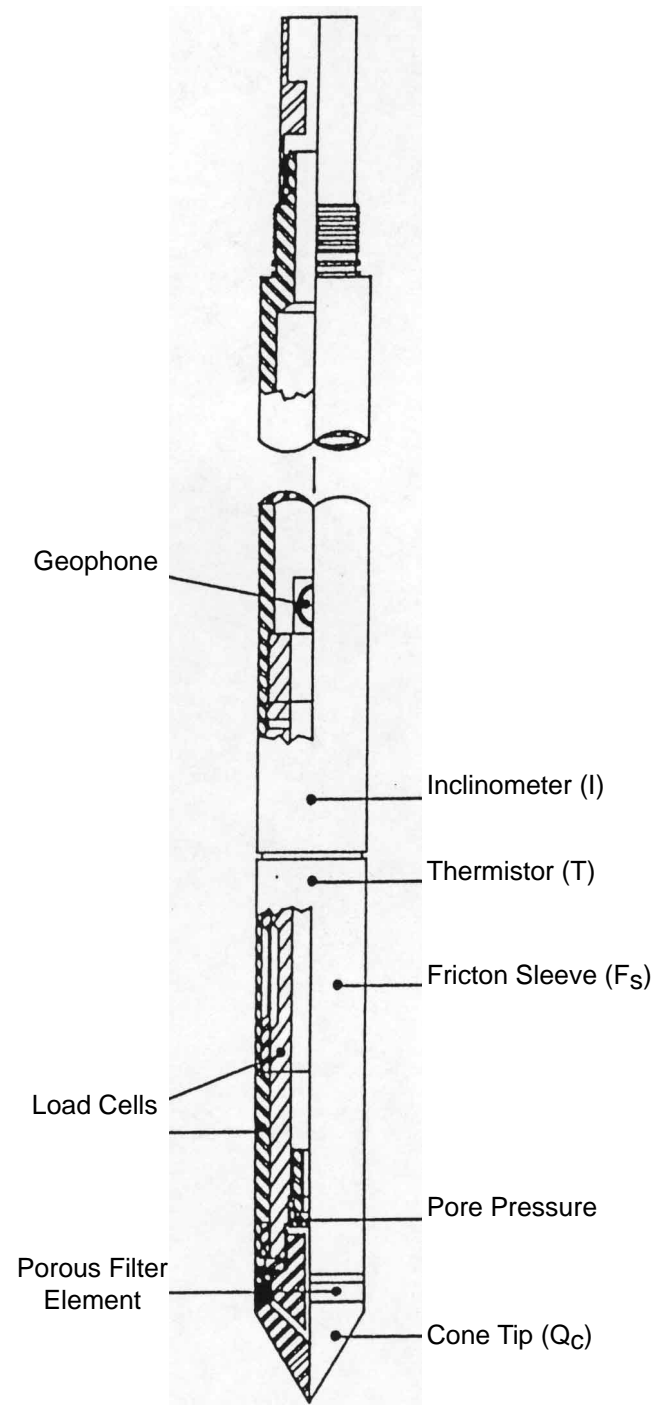


Figure 1. Seismic cone penetrometer

Most cones were pushed to a minimum depth of 35 m or more; however, several cones met with shallower refusal (resulting from encountering a firm layer- an indirect indication of the top of Pleistocene materials, in this delta setting).

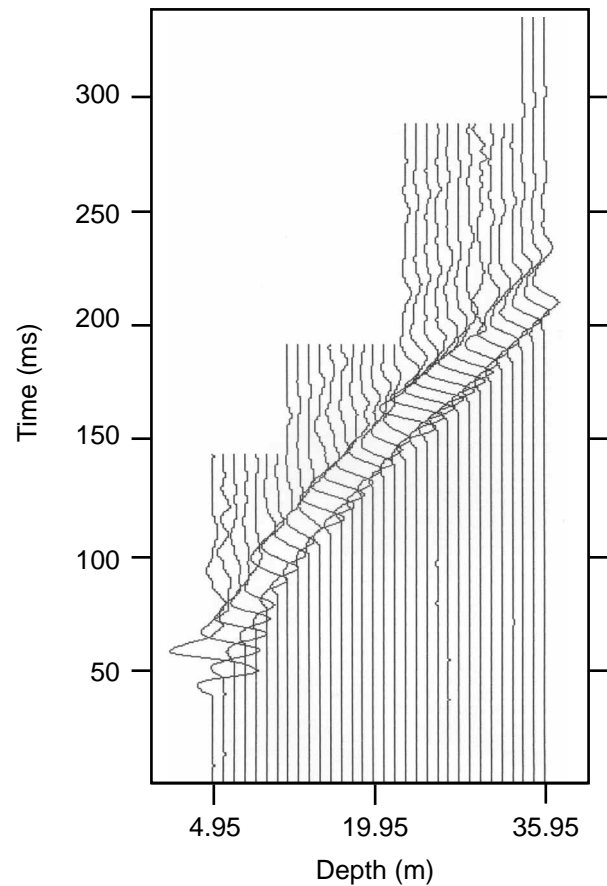


Figure 2. .SCPT95-1



## BOREHOLE SHEAR WAVE VELOCITY LOGS

Surface-to downhole shear wave velocity measurements were made in over 40 boreholes drilled by GSC in the Fraser River delta. Most of these boreholes were drilled for geotechnical or geological investigations, and were subsequently cased with 50mm or 63 mm ID PVC casing. At most sites, the PVC casing was not grouted, but rather, sand fill was poured between the outside of the casing and the borehole wall; usually 6 months to a year elapsed before shear wave velocity measurements were made, allowing time for borehole wall slumping to occur so that good casing-to-formation coupling was achieved. Some boreholes were properly grouted to the formation using standard grouting cement procedures (e.g. BCHWYS-ANNICIS, FD92-11, FD94-3, FD94-4, FD95-S1, FD96-1, FD97-1, FD97-2, FD97-3, FD97-4, FD97-5, FD97-6, FD97-7). Completions in this manner allowed almost immediate access to these boreholes for downhole shear wave velocity measurements.

Most pre-1994 downhole shear wave velocity surveys utilized in-house GSC equipment consisting of a OYO BOREHOLE-PICK 3-component well-locked geophone sonde. This device used orthogonal 8-hertz geophones in a pressure-sealed case which was locked to the borehole wall using an inflatable rubber bladder mounted on one side of the case. The advantage of this tool was its “slim-hole” installation in a 50 mm ID PVC casing (using low-cost off-the-shelf thin-walled schedule 40 jointed tubing). The major disadvantage of the device was the lack of orientation of the borehole sonde, and its tendency to rotate position when moved between locations in the borehole.

Since 1994, most borehole surveys were conducted with somewhat larger diameter oriented 3-component borehole sondes, requiring 63 mm ID casing. Two types were employed: 1) a sonde manufactured by Frontier Geosciences Inc. of Vancouver, consisting of a spring-loaded pressure-case, with 8 Hz orthogonal geophones, designed for use in slotted-PVC casing, and 2) a sonde manufactured by GEOSTUFF Inc of San Francisco, a bow-spring-loaded pressure-case 3-component 8-Hz sonde with magnetic compass orientation.

For boreholes where the Frontier Geosciences unit was used with slotted casing, borehole inclinometer and rotation measurements were also conducted in order to correct for rotation of the slotted casing with depth (boreholes FD92-11, FD95-S1, FD95-4). The Frontier Geosciences unit was also used in non-oriented configuration in boreholes FD-94-3, FD94-4 and FD96-1.

Most other post-1994 boreholes were surveyed with the GEOSTUFF Inc sonde. For these holes, thin fiberglass rods were attached to the sonde allowing the operator to rotate the sonde from ground surface to a preferred orientation for each location in the hole (it was found that +/- 2 degree accuracy could be maintained to a depth of 100 m using this system).

In all cases where borehole sonde orientation was maintained, data quality was far superior to

that of non-oriented holes. This was mainly due to alignment of the polarized surface shear wave source with one particular horizontal geophone component (hence polarity reversals of a particular horizontal component due to sonde rotation was eliminated and post-aquisition vector rotation processing was not necessary).

The seismic source used for all borehole shear wave work consisted of a truck-loaded I-beam struck sequentially on each side with a 7.5 kg hammer. An electronic trigger switch was mounted on the hammer to give source impulse time zero to within  $\pm 0.1$  ms accuracy. By hammering on one side of the I-beam, polarized shear motion was generated (generally the orientation was “towards” or “away” from one of the horizontal geophone components of the sonde). Although equal numbers of “towards” or “away” polarized stacks could be summed together on a stacking seismograph to minimize other signal-generated noise, the GSC field procedure was to record individually the unidirectional polarized stacks (e.g. two seismic records “towards” and “away” for each downhole sonde position), and to compare (or sum) these two records during computer processing.

During the several years of borehole seismic recording, various types of digital stacking engineering seismographs were used, including, the EGG-1210F, Bison-9000, and the Geometrics R-24 Strataview. Recording dynamic range varied between 10-bits to 16-bits+, however, signal-to-ambient noise was seldom a problem. Stacked hammer blows varied between 3 near surface to as much as 10 at 100+ metres depth.

Most boreholes were surveyed using a 1 metre vertical separation between sonde locations. At some locations (e.g. where the borehole had been drilled only a few meters into the top of the Pleistocene strata), the sonde spacing was reduced to 0.5 metres to ensure adequate delineation of potential velocity boundaries.

Onset of shear wave energy in borehole seismic records was identified through a combination of examination of each of the polarized records for a borehole sonde position, particle-motion plotting, and examination of composite depth record sections of individual horizontal geophone components.

Shear wave travel times were plotted, and examined to identify depth-zones where closer re-analysis was warranted. The edited travel-time-depth data was processed using a 3-point to 12-point running least-squares fit to obtain downhole interval velocities. The processed data, shown on the plots give also  $\pm 1$  or 2 standard error bars derived from the least-squares fits. These error values should only be used as a guide to the relative “goodness” of a velocity fit, since the standard deviation, associated with a standard error derived from only a few data points, is quite large. The “error bars” indicate either uncertainty in the travel-time picks or small-scale vertical variations in shear wave velocity within the least-squares fitting window.

Some specific boreholes were examined for “shear-wave splitting” or horizontal velocity anisotropy (boreholes FD92-11, FD95-S1, and FD95-4) which might be related to horizontal



# FRASER DELTA SITE 70 (BH94-3)

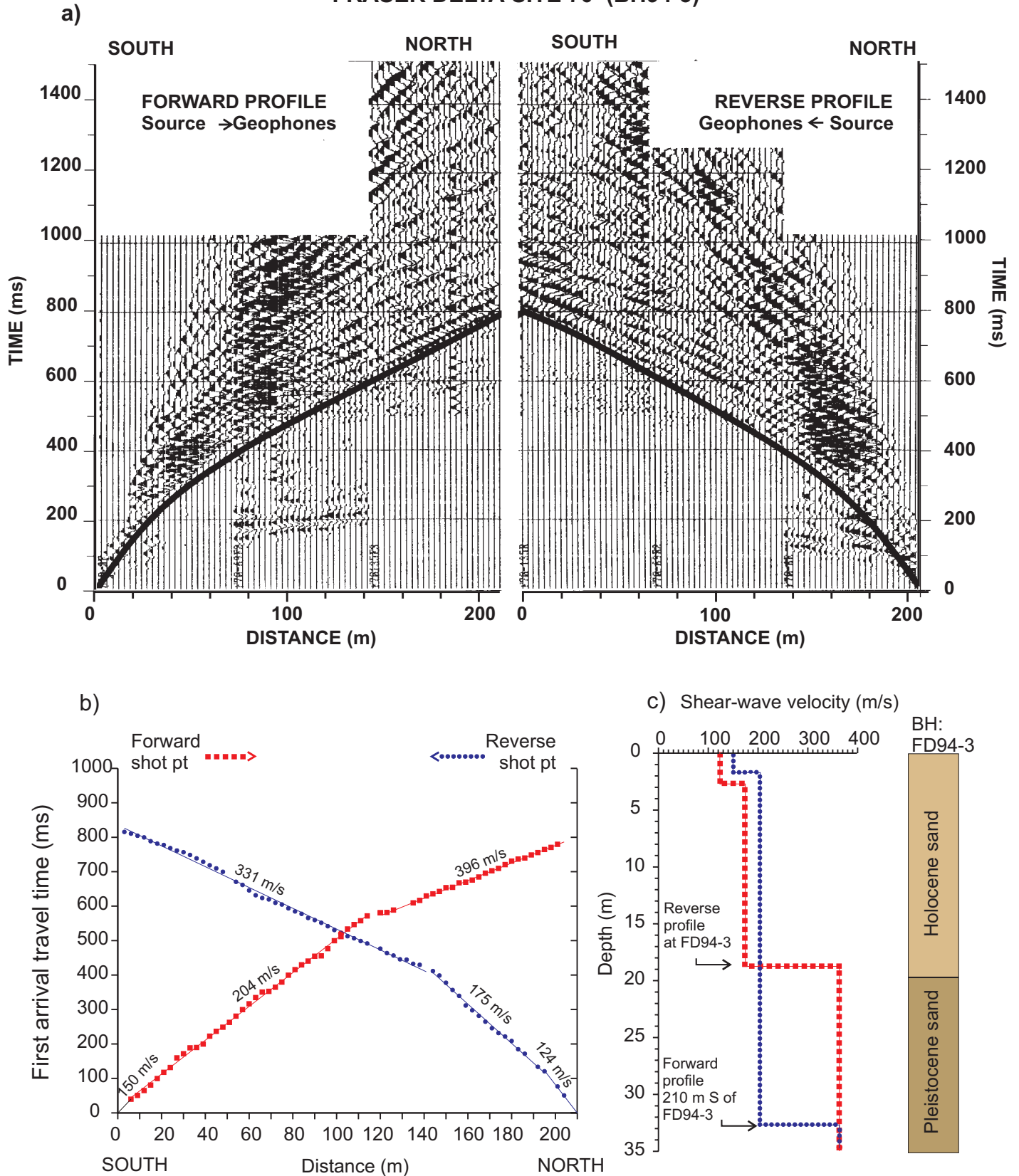


**Figure 1. Reversed shear wave refraction spread at borehole FD94-3 (See refraction site 70). a) Composite record suite (geophones in transverse orientation). B) First arrival time-distance plot. C) Layered depth determination compared to borehole geology.**

stress anisotropy. Hence the downhole experiments included two orientations of the horizontal surface source as well as the “forward” and “away” seismic records. The travel-time and velocity depth plots shown for these holes are composites of all the directional data recorded, although the “error bars” reflect the directional variation. The reader is referred to Harris et al.(1996) for a detailed description of the experiment and the results obtained.

The number of data points used in the running least-squares velocity fitting routine applied to the travel-time-depth data of individual borehole holes was varied between 3 and 12 (e.g. in most cases, the data window varied between a vertical distance of 3 and 12 m). A specific n-point velocity fit was selected for display for each of the boreholes; this selection was based on the relative size of “error bars” compared to the vertical velocity variations obtained and was designed to show the major velocity structure within the borehole. The user may wish to apply differing “windows” to the travel-time-depth data (by accessing the data in the **DATAROOM DIRECTORY**). It is well-known that a “box-window” running least-squares fit can produce “side-lobe” wavelength aliasing to the velocity-depth results. In order to examine this phenomenon, Fejer-weighted (triangularly weighted) least-squares windows have been applied to some of the borehole data sets (e.g. FD94-3, FD94-4, FD-95-S2). In these cases, “error bar” size increased, however no significant side-lobe wavelength differences were observed; hence the “box-window” approach was maintained throughout for all boreholes.

Using a running least-squares fit however, smoothing of vertical velocity variations, associated with the length of the data window will indeed occur. Alternative interpretational approaches to the travel-time-depth data are certainly valid, and could be applied for specific goals. For example, the data could be interpreted using straight-line velocity segments; Hunter et al.(1997) applied this technique, along with the “reduced travel-time” approach, for the precise delineation of velocity boundaries in some boreholes in the Fraser River delta. The user is encouraged to re-examine the travel-time data using such alternative techniques.

## SHEAR WAVE REFRACTION METHODS

The shear wave refraction methodology applied to sites in the Fraser River delta consisted of “true reversed” refraction sounding (Telford et al., 1976), a standard procedure wherein seismic source points are fixed at either end of an array of geophones. This type of geometry allows one to detect the presence of dipping subsurface layering and to correct for apparent velocities.

To obtain horizontal motion associated with shear wave refractions, 8 Hz horizontal geophones were used. The geophones were arranged in SH mode (i.e. the axis of the geophone coils were perpendicular to the line of the geophone array); this was done to minimize any P to SV (radial shear mode) converted wave energy which would be considered as signal-generated noise.

For most shallow depth soundings (<40 m depth), a polarized horizontal shear wave source was used; This consisted of a loaded I-beam hammered sequentially in both directions perpendicular to the line of the array; This technique produced reversing polarized SH mode refractions which were used to identify the onset of shear energy in the presence of noise.

For some soundings reaching to depths of 100 m or more (by using geophone arrays in the range of 300 to 600 m length), a standard 8-gauge in-hole shot-gun source was used; although this source is an explosive one, it produces equal amounts of P and S energy (without the capability of polarity reversal).

At some site locations, it was not logistically possible to shoot reversed spreads, since the urban environments sometimes restricted full deployment of the arrays. Hence only the travel-times and shear wave velocities are shown for a single-ended array.

A composite suite of forward and reverse field records, shear wave travel-time interpretations and velocity depth structure is shown in Figure 1.

The onset of shear wave refractions were manually picked from the raw field records for all sites. The travel-time-distance data from the forward and reverse composite arrays were examined separately.

Two similar velocity-depth interpretation schemes were used for each travel time-distance set: the conventional “layered-case” interpretation, and a computer-fitted “velocity-depth” routine.

The “layered-case” interpretation requires an interpreter to examine the travel-time-distance data and to divide the data into straight-line segments. The slopes of the line segments, as well as the zero distance intercepts of each of the line segments are used to compute layer thicknesses and shear wave velocities (using standard equations given by Dobrin (1960), or Telford et al. (1976). Interpretations done in this manner are noted as “Layered interpretation” on the velocity-depth plots of each site.



The “velocity-depth” computer routine uses a “hands-off” approach, whereby a 5-point running least-squares fit is applied along the travel-time-distance curve centered at each of the data points. The computer routine (after Hunter, 1971) applies a smoothing function to the data, to account for record-picking errors. Essentially, each data point is associated with a straight-line velocity segment which is treated in a similar manner to the “layered case” interpretation; if shear wave velocities are increasing uniformly with depth, then the routine will compute velocity-depths associated with each data point. If a well-defined straight-line velocity segment (associated with a thick layer of uniform velocity) is detected, then the routine will preserve the velocity segment and treat it as a thick layer in the analysis (to within certain velocity variation limits as defined by the interpreter). The advantage of this routine over that of the “layered-case” analysis is that the data does not need to be divided into velocity-segments, which may vary considerably between interpreters. As well, the “velocity-depth” routine gives an indication of the vertical velocity resolution (or lack of) between successive travel-time-distance data points. Although the routine is “operator hands-off” the input parameters governing the degree of data smoothing is defined by the interpreter, and does affect the overall velocity-depth interpretation. Hence the output is, by no means, free of interpreter bias.

The first arrival shear wave data is presented in the form of a travel-time-distance plot showing both forward and reverse data on the same plot. The user is encouraged to follow directions to the **DATAROOM** directory indicated to obtain the digital data and perform his own analysis.

The velocity-depth interpretations for the forward and reverse profiles at each site are shown as separate plots. Each plot shows both the “Velocity-depth” and the “Layered” interpretations. At most sites, both interpretation techniques show correlatable results, with the “Layered” interpretation being conservative for maximum depth of penetration (an interpreter bias - all sites were interpreted by the same person).

For interpretations done using the “Layered” technique, where dipping layers were apparent from inspection of the forward and reversed travel time-distance curves (e.g. top of high velocity Pleistocene), an arithmetic average shear wave velocity (from the forward and reverse plots) was used in the calculations of depths to that horizon.

## METHODS OF COMPUTING COMPRESSIONAL AND SHEAR WAVE INTERVAL VELOCITY DATA FROM MULTICHANNEL SEISMIC REFLECTION SURVEYS

To date, there is a paucity of direct shear wave velocity measurements for deep soil profiles within the delta, due mainly to the extreme thickness of the unconsolidated Quaternary sediments and lack of deep geological-geotechnical boreholes. Recent surface shear wave seismic refraction surveys and geotechnical drilling (Dallimore et al., 1995; Luternauer and Hunter, 1996) are beginning to address the problem and are providing shear-wave velocity information to depths of 300 m. However, the average thickness of unconsolidated overburden in the Fraser River delta is in the order of 500 m, with some areas exceeding 1000 m (Britton et al., 1995). No direct measurements of shear wave velocities of the lower Quaternary sediments or the Tertiary sedimentary rock have been made.

It is possible, however, to estimate the shear wave velocity-depth profiles within the delta from a knowledge of the compressional wave ( $V_p$ ) velocity structure, where such information is available.

Over the past several years, Dynamic Oil Ltd., of Vancouver, has acquired a data bank of multichannel seismic reflection survey lines within the delta area, as part of an on-going program of hydrocarbon exploration. Approximately 126 line-kilometers of 120 channel, 120-fold "common-depth-point" seismic data have been obtained at a geophone group spacing of 17.5 m using vibroseis sources (Britton et al., 1995), which provide relatively detailed seismic stratigraphic structure (including depth to top of Tertiary bedrock) along regional lines. Routine



Vibroses seismic sources used to obtain deep seismic reflection data in the Fraser delta

computer-based seismic compressional wave ( $V_P$ ) velocity analysis methods have been applied to selected seismic records at intervals along each of the seismic survey lines in order to process the data in the form of seismic reflection sections. The output of such analyses, called “velocity panels” give the average compressional wave velocities down to reflections

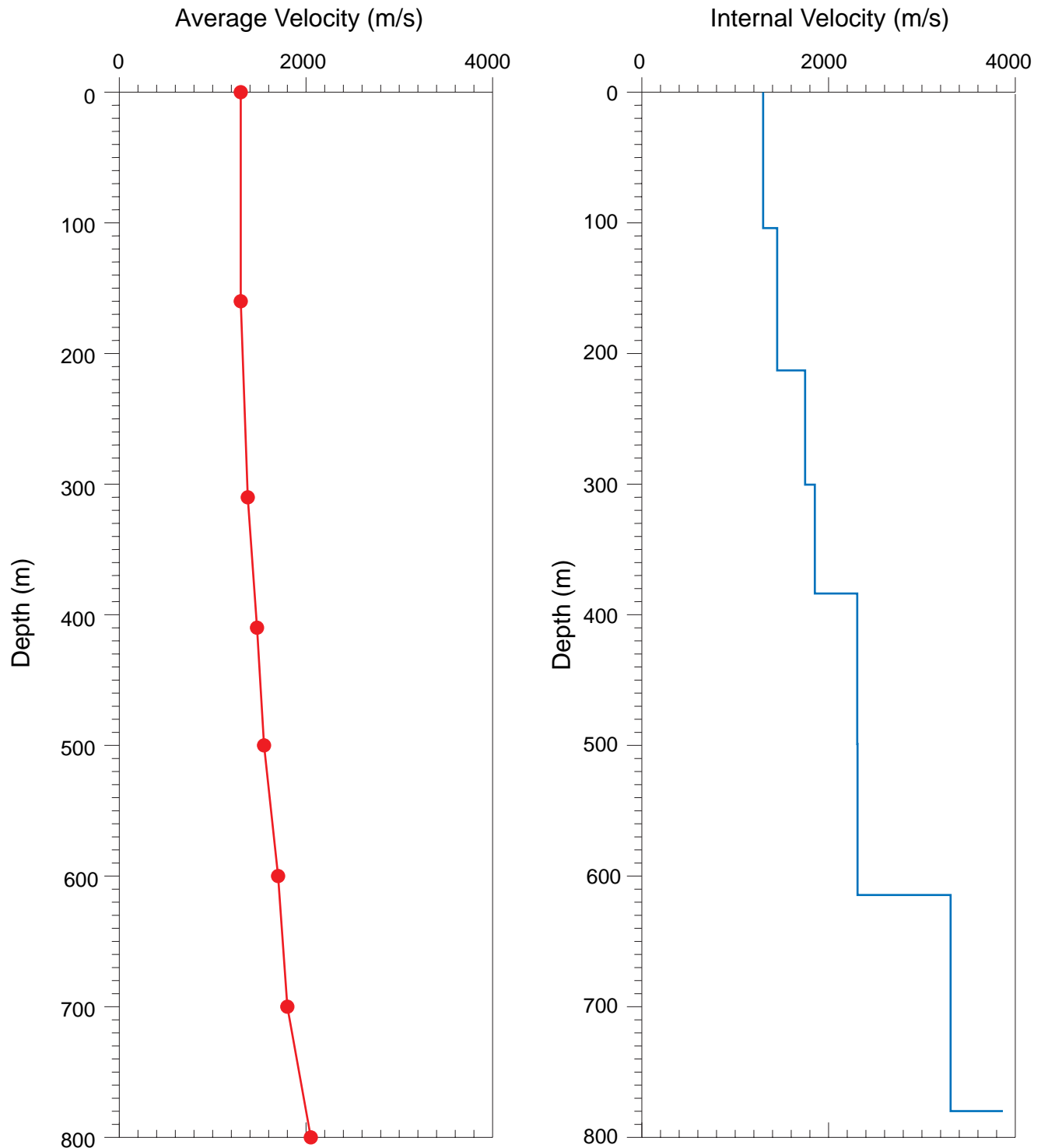


Figure1. Example average velocity vs 2-way travel-time compressional wave velocity panel (left hand side) and the derived compressional wave interval velocity vs depth interpretation (right hand side) for velocity panel # 16 from seismic survey line W89-07.

interpreted from the seismic records. Hence the velocity panels are a tabulation of the two-way travel-time of the compressional wave reflected from seismic boundaries ( $V_P$  velocity discontinuities usually associated with sediment lithology changes) along with the average compressional wave velocities.

The locations of Dynamic Oil's seismic survey lines and the 183 velocity panels available within the Fraser River delta are shown on the location map. The UTM co-ordinates of each velocity panel were measured from 1:50,000 scale shot-point location maps of Dynamic Oil Ltd., and are given to an approximate accuracy of  $\pm 50$  m.

The two-way reflection travel time, along with the average compressional velocity information contained in a velocity panel can be interpreted in the form of seismic velocity layering, using routine processing techniques to obtain "interval" compressional wave velocities and thicknesses of each of the seismic layers. An example is shown in figure 1.

$V_P/V_S$  ratios have been utilized for many years as an investigative tool in the delineation of hydrocarbon reservoirs in sedimentary rocks, and a wealth of laboratory and field data are available for that geological environment (Nur and Wang, 1989). As well, extensive investigations of  $V_P/V_S$  have been carried out for various types of marine sub-bottom sediments (Hamilton, 1979). There does not appear to be an extensive data set in the published literature for Quaternary on-land sediments. However, the above-mentioned studies can serve as a guide in the establishment of  $V_P/V_S$  relationships within the Fraser River delta.

Figure 2 shows established  $V_P$  vs  $V_S$  relationships from laboratory and field observations for clastic silicate rocks (Castagna et al., 1985), for clayey sandstones (Han et al., 1986) and fine-grained unconsolidated marine sediments of terrigenous origin (Hamilton, 1979). These curves represent guidelines for the Fraser delta sediments; however, none of the established relationships should be expected to relate directly to Holocene deltaic sands and silts, or to Pleistocene glacially-derived sediments.

Compressional and shear wave velocities were recently measured in two 300 m deep boreholes in the Fraser delta (Dallimore et al., 1995) that encountered both Holocene and Pleistocene sediments. Before using these  $V_P$  and  $V_S$  velocities in developing an empirical  $V_P/V_S$  relationship, the data were carefully inspected and data points were discarded in areas of the boreholes where there were indications of gas in the pore space (small quantities of interstitial natural gas can substantially reduce the measured compressional wave velocity from its value at 100% pore-water saturation, see Brandt, 1960). The remaining 260 data points from boreholes FD94-3 and FD94-4 are shown in Figure 3; these data help to establish the  $V_P/V_S$  relationship for compressional wave velocities between 1500 m/s and 2200 m/s. However, since the lower portion of the Quaternary section, as well as the upper portion of the Tertiary bedrock in the Fraser delta have compressional wave velocities in the 2000-3000 m/s range, it was thought necessary to search for additional relevant data. Reilly (1994) has published borehole measurements of Tertiary (and younger) clastic rocks from the North Sea area. A total

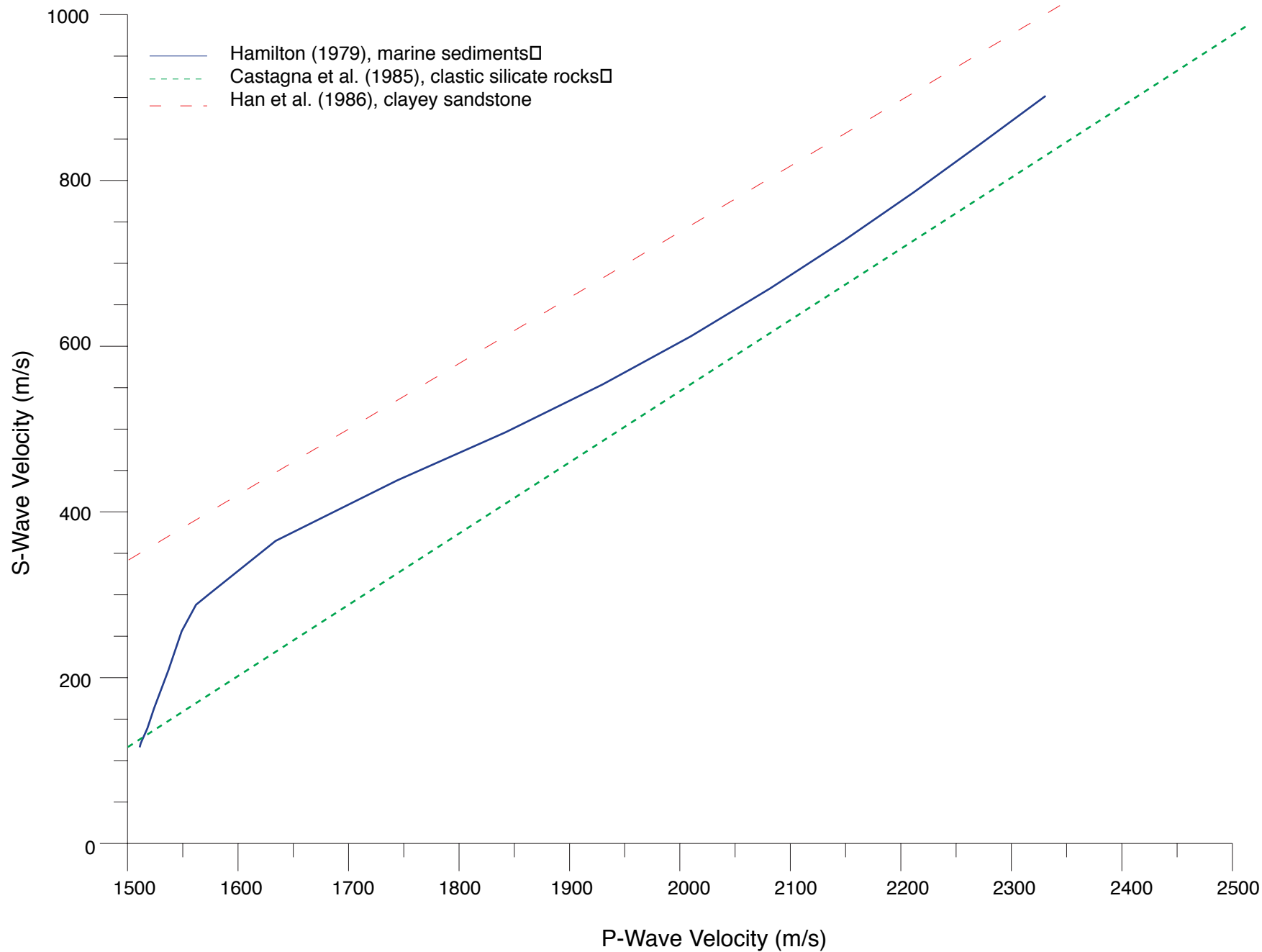


Figure 2. Previously published shear wave velocity ( $V_s$ ) vs compressional wave velocity ( $V_p$ ) relationships for sediments and sedimentary rocks.

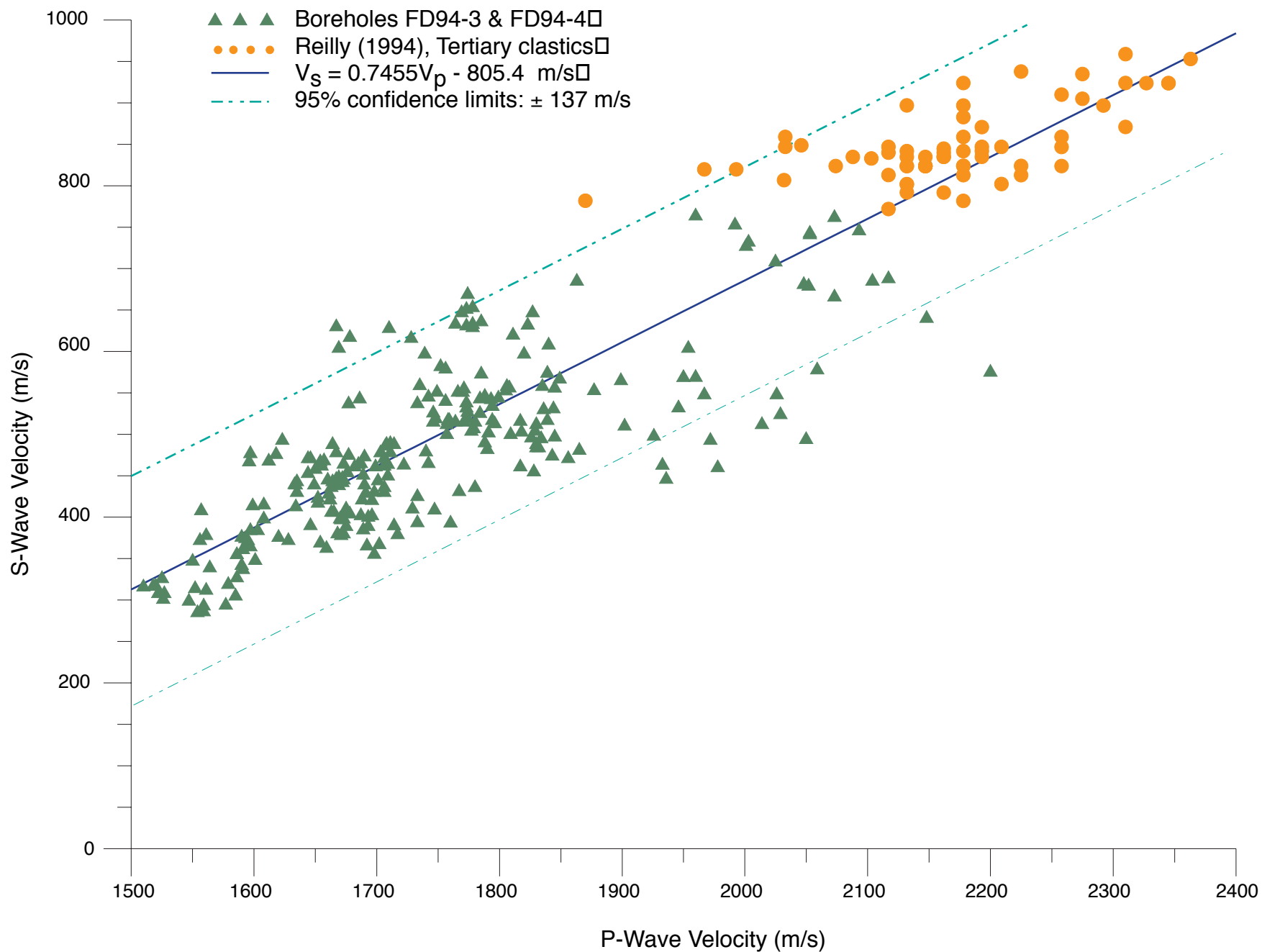


Figure 3. Combined  $V_P$ - $V_S$  data from Fraser delta boreholes in Quaternary sediments and Reilly's (1994) North Sea boreholes in Tertiary clastic sedimentary rocks.



of 64  $V_P$  and  $V_S$  measurements from Eocene and Paleocene clastic rocks in the depth range of 1000 m were obtained from the published borehole logs and added to the plot shown in Figure 4. It is suggested that these measurements may be the most representative data available for the upper Tertiary sedimentary bedrock in the Fraser River delta, at similar depths of burial.

A linear least-squares fit of the combined Fraser delta borehole data (FD94-3 and FD94-4) and Reilly's (1994) Tertiary data (as shown in Figure 3) leads to the following relationship:

$$V_S = 0.7455V_P - 805.4 \text{ m/s} \quad \dots\dots\dots(1)$$

with a standard deviation of  $V_S$  on  $V_P = 68.5 \text{ m/s}$

Figure 4 shows the data of this study compared to the established curves of Hamilton (1979), Castagna et al. (1985) and Han et al. (1986). The relationship given by Castagna et al. (1985), known as the "mudrock line" for "clastic silicate rock composed primarily of clay- or silt-sized particles" is as follows:

$$V_S = 0.8621V_P - 1172.4 \text{ m/s} \quad \dots\dots\dots(2)$$

The relationship given by Han et al. (1986) for shaly sandstones is:

$$V_S = 0.7937V_P - 849.2 \text{ m/s} \quad \dots\dots\dots(3)$$

The marine sediment relationship of Hamilton (1979) (see also Fig.4) for terrigenous materials "mostly silt-clays, turbidites, mudstones, shales" to depths of 1000 m below seafloor, is a composite of four regression equations:

for  $V_P$  between 1512 and 1555 m/s:

$$V_S = 3.884V_P - 5757 \text{ m/s} \quad \dots\dots\dots(4a)$$

for  $V_P$  between 1555 and 1650 m/s:

$$V_S = 1.137V_P - 1485 \text{ m/s} \quad \dots\dots\dots(4b)$$

for  $V_P$  between 1650 and 2150 m/s:

$$V_S = 991 - 1.136V_P + 0.47V_P^2 \text{ m/s} \quad \dots\dots\dots(4c)$$

for  $V_P$  greater than 2150 m/s:

$$V_S = 0.78V_P - 962 \text{ m/s} \quad \dots\dots\dots(4d)$$

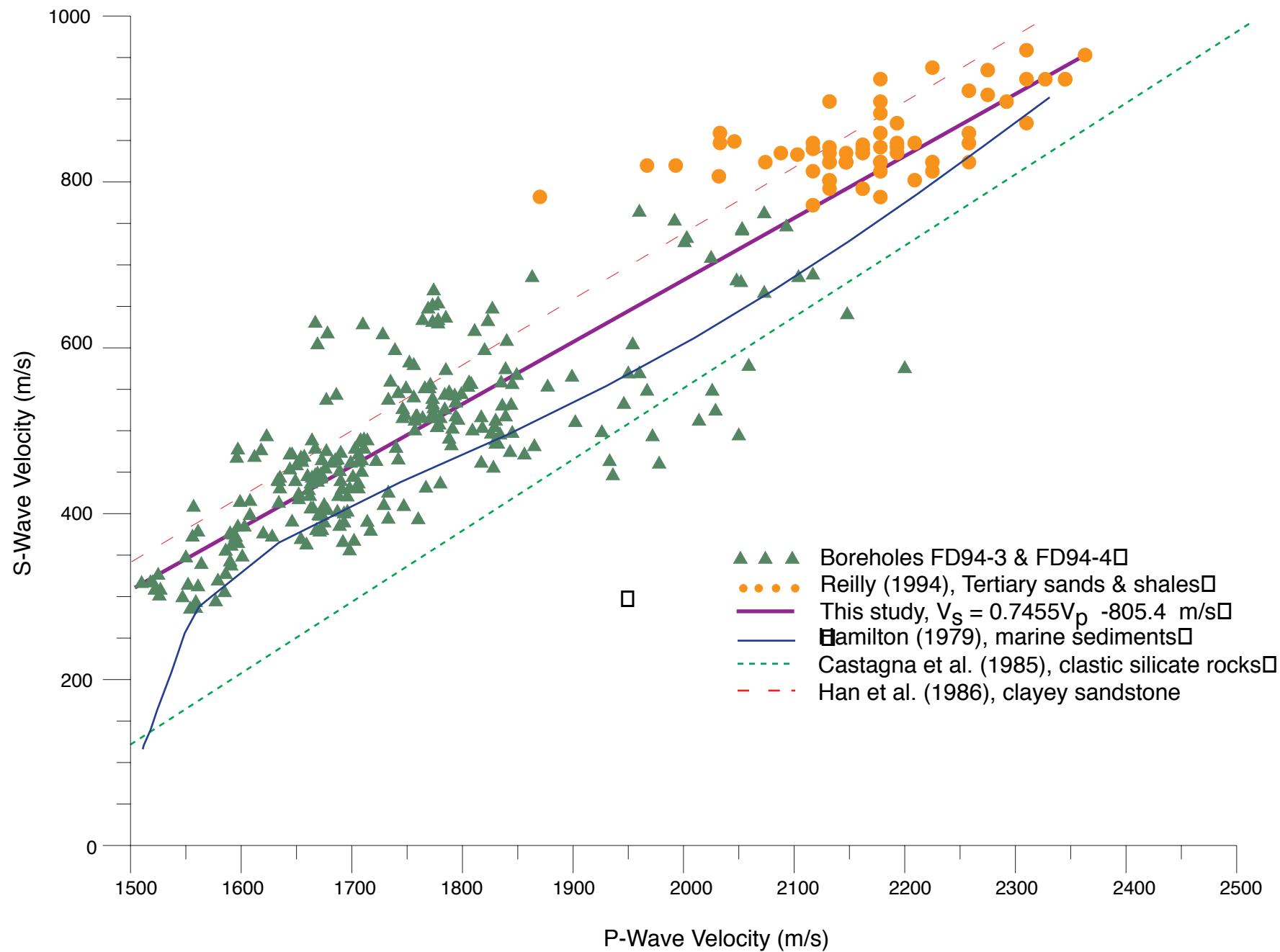


Figure 4. Comparison of the  $V_p$ - $V_s$  data from this study with previously published relationships.

Much of the non-linearity of Hamilton's relationship results from large increases in shear wave velocities in the first 50 meters below sea-bottom, probably resulting from decreasing porosities due to sediment loading. With respect to the Fraser delta data, most data points were obtained at depths beyond 50 meters; furthermore, the application of the empirical relationship is directed towards the deeper portions of the Quaternary section; hence an empirical fit invoking a polynomial expression for low  $V_P$  velocities was not pursued. However, in future, when more shallow borehole  $V_P$  and  $V_S$  data becomes available it may be possible to obtain well-defined relationships for near-surface Holocene deltaic sediments.

The relationship between the  $V_P/V_S$  ratio and compressional wave velocity  $V_P$  is shown in Figure 5 for the Fraser delta (equation 1) along with the previously cited models (equations 2 to 4). It is interesting to note the convergence of  $V_P/V_S$  ratios for all models at high compressional wave velocities ( $>2000$  m/s). Hence for the Tertiary bedrock in the Fraser delta,  $V_S$  estimated from  $V_P$ , using any of the above curves, should give values within approximately 10-15% of one another.

The two-way travel time and average compressional wave velocity data from each of the velocity panels of Dynamic Oil's seismic reflection data were analysed to obtain interval compressional wave velocity- depth layering using standard methods (Dix, 1955). Equation 1 was used to estimate the shear wave interval velocity layering. The interval velocity-depth interpretation for both shear and compressional waves are shown in a single plot per velocity panel, along with the interpreted top of Tertiary bedrock (after Britton et al., 1995). The error envelopes for the shear wave velocity interpretation represents  $\pm 2$  standard deviations (95% confidence limits).

As noted above, the presence of small quantities of natural gas in the pore spaces of sediments or rock may result in a large decrease in the observed compressional wave velocity  $V_P$ . This can lead to incorrect estimates of  $V_S$  using any of the established relationships (shear waves are transmitted through the granular framework and are not affected by variations in pore-fluid contents). In near-surface unconsolidated overburden, the presence of gas is evident where  $V_P$  velocities are less than that of water ( $<1460$  m/s). Within the lower Quaternary section or within Tertiary bedrock, the presence of gas may be indicated by a velocity reversal with depth. Without independent information on gas content within the section, it is not possible to define areas where the estimated  $V_S$  velocities have been effected by abnormally low  $V_P$  velocities. **The user of this information is cautioned to inspect the plotted  $V_P$  interval velocities for such low  $V_P$  velocities or velocity reversals with depth, and in these cases to use the estimated  $V_S$  velocities only as a guide to the lowest possible value in that depth interval.**

The depth position to the top of the Tertiary bedrock, shown on each of the plots, is taken from the interpretation of Britton et al. (1995). On many of the plots, there appears to be a good correlation between the interpreted top of Tertiary and a large velocity increase in  $V_P$ , as might

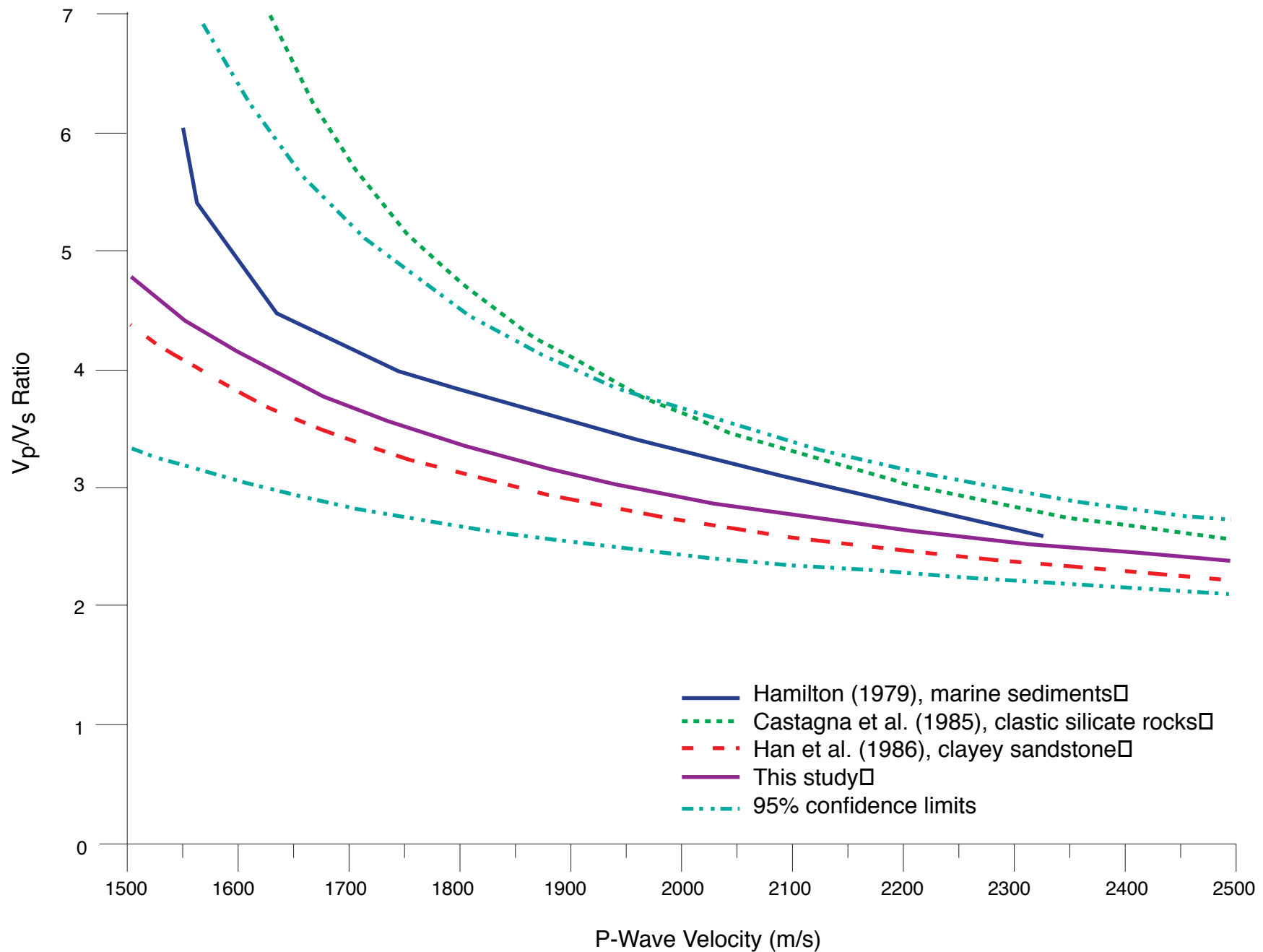


Figure 5.  $V_p/V_s$  ratio vs compressional (P) wave velocity. Note that all models lie within the 95% confidence limits of this study for  $V_p$  values.2000m/s.

be expected. In several plots however, the interpreted top of bedrock is shown to be either above or below such a large contrast, sometimes by as much as 100 m. Possible explanations of the discrepancies are as follows:

1) Depths interpreted by Britton et al. (1995) were derived from two-way travel time reflection picks at approximate 170 meter horizontal distances along the seismic section. The P wave reflection interpreted as the top of bedrock often appears as an angular unconformity shown in the seismo-stratigraphy (Figure 2 of Britton et al., 1995), and trace to trace correlation along the seismic section can be done with confidence. Where reflectors are parallel and flat-lying, the velocity panel data were used as a guide in the interpretation. Conversion to depths was done through development of a “delta-wide” least-squares fit polynomial curve of two-way travel time vs depth derived from all 182 velocity panels (Figures 5,6,&7 of Britton et al., 1995), with a relatively large statistical error as stated (e.g. 68% confidence limits for a depth of 500 meters is approximately +/- 50 m and for a depth of 1000 m is +/-80m). Hence many of the discrepancies between top of Tertiary from Britton et al (1995) and the large velocity contrasts shown on the plots in this report are within the 1 or 2 standard deviation error limits given.

2) As well, on plots where the interpreted top of Tertiary occurs at depths below a large velocity increase, it is suggested that high  $V_P$  velocities possibly could exist in the basal Pleistocene section associated with overconsolidated sediments, and the velocity contrast across the Pleistocene -Tertiary boundary may be small in comparison to the large contrast occurring at a somewhat shallower depth. High  $V_P$  velocities have been measured in Pleistocene materials in the delta (Dallimore et al., 1995; Hunter, unpublished borehole data from FD96-1).

Although the present authors have no ready access to statistical data associated with the processing steps taken to compute the  $V_P$  interval velocities, it is suggested that the reflection velocities derived from the field data acquisition geometry described, as well as the modern computer analysis techniques employed (Hubral and Krey, 1980), are probably accurate to within +/- 10%. A further indication of the original data quality used for processing velocities can be inferred by the number of reflection layers indicated on the plots. Each interpreted velocity layer indicates that a reflection was identified and processed with sufficient signal-to-noise ratio to obtain a velocity estimate. Hence, we suggest that the  $V_P$  velocities used in this analysis are well-determined and are a reasonable approximation of the true velocity structure of the Quaternary and upper Tertiary bedrock materials in the Fraser River delta..

Derived shear wave velocity structure as shown on the plots indicates the presence of large velocity contrasts at depth (often x2 to x3), usually associated with the interpreted Quaternary-Tertiary boundary (after Britton et al., 1995). In some cases, large velocity contrasts also occur within the Quaternary section at shallow depths; these may be associated with Holocene-Pleistocene boundary, however, no independent correlateable geological evidence is available. Should this data be utilized to develop shear wave velocity structure models (or small strain

$G_{\max}$  models) for earthquake ground motion response, the user is cautioned that the vertical shear wave velocity resolution (thickness of velocity layers) is relatively coarse; this in turn may define the high frequency (short period or wavelength) limit of such models.



## BOREHOLE GEOPHYSICAL METHODS

Over 40 boreholes have been drilled by the GSC for geological-geophysical delineation of Quaternary stratigraphy in the Fraser delta. Almost all of these holes were cased with 5-6.5 cm diameter PVC pipe for the purposes of geophysical logging using standard techniques. Most of these holes have also been preserved with steel surface casing protection for future testing of new geophysical downhole techniques. Access to these holes for the purposes of testing new techniques by applied research organizations may be possible; please contact the authors of this open file for details.

Three passive logs run in these holes using the Geonics EM-39 logging system are: natural gamma, inductive electrical conductivity, magnetic susceptibility. As well, many of the holes have been preserved for future testing of new geophysical downhole techniques.

### Natural Gamma Log

The natural gamma log measures the gamma radiation from radioactive isotopes of potassium (K), uranium (U), and thorium (Th) which occur naturally within unconsolidated sediments. The changes in relative total count response in a borehole can be used as a qualitative estimate of sediment type. Within the sediments of the Fraser River delta, coarse grained sediments (sands) yield relatively low gamma count rates, whereas fine grained units (silts and clays) give higher count rates, often a factor of 2 higher than that of coarser sediments.

The overall level of the natural gamma response measured by the borehole sonde is strongly dependent upon the particular tool (i.e. the type and sensitivity of the detection electronics) and also on the borehole diameter (for many types of equipment, the majority of the measured gamma response comes from a circumjacent radius of 0.5m or less). Hence for qualitative geological interpretations within a borehole, or for borehole-to-borehole correlatable interpretations, similar borehole (diameter and casing) conditions, as well as sondes, should be maintained throughout the survey area. Within the Fraser delta survey area, most GSC boreholes were drilled with similar diameters and were completed with similar PVC casing size and wall thickness; as well, most holes were logged with the same borehole gamma sonde (Geonics EM-39G.). As a result, hole-to-hole qualitative geological interpretations can be made. In a few cases, where different sonde types were used, careful in-hole calibration of the sondes were made over a wide variation of lithological responses in order to adjust overall response levels to the above-mentioned "standard" sonde type.

An additional factor governing the overall response of the natural gamma tool is the combined effects of the integration rate of the electronics, the background noise response (ambient and instrumental) and the vertical logging speed. At the onset of the borehole logging program in the delta, a high integration setting was chosen for the work (5 second time constant - a measure of the electronic integration of the measured number of received gamma rays); this in turn dictated a slow vertical logging speed of 2.5 cm/s which has been maintained throughout,

in all boreholes. Further, since radioactive decay and emission of gamma rays are temporally random, measurements were made with the sonde stationary over long periods of time in various sediment types to determine the statistical variations. An average combined temporal and instrumental error assigned to Fraser delta gamma logs is a 2 standard deviation variation of  $\pm 6.5$  counts/sec (95% confidence limits) over the observed count rate range. In effect, this number dictates the limit of vertical resolution available for qualitative geological interpretations (e.g. the definition between thin sand and silt bands). To date all published GSC borehole gamma logs obtained in the Fraser delta have been presented in such a "raw" format with no additional post-acquisition digital filtering or smoothing applied.

Compilation of natural gamma logs from GSC boreholes in the Fraser delta are given by Hunter et al (1994), Dallimore et al (1995), and Dallimore et al. (1996). Geological interpretations utilizing this data include, Clague et al (1998), Monahan et al, 1993, Christian et al. (1998), Christian et al., 1995).

In general, the surface layer throughout the delta consists either bog and lacustrine deposits, sandy distributary channel materials, and fine-grained overbank deposits (Armstrong, 1984; Monahan et al, 1993) to a depth of 1-8 m; the fine grained units are manifested by relatively high gamma count rates.

Beneath the surficial units, a Holocene delta-wide sand sheet has been identified (Monahan et al, 1993) and is typified by relatively low gamma count rates. The boundary between the surficial unit and the sand sheet is often gradational with one or more fining-upwards sequences identified on the gamma logs.

Beneath the delta sand sheet, a thick unit of mainly fine-grained materials (silts and clays) are interpreted to be Holocene foreset and prodelta sediments (Clague et al., 1991) which may extend to depths in excess of 300 m (Dallimore et al., 1996). This sequence yields high gamma count rates; increasing count rate with depth within this combined unit can be associated with increasing fines content.

The Holocene-Pleistocene boundary at the base of the deltaic sediments is often delineated by an abrupt break in the gamma count rate associated with a lithological discontinuity (e.g. Holocene clayey silt overlying Pleistocene diamicton) (Dallimore et al., 1995, Dallimore et al., 1996).

### **The Electrical Conductivity Log**

The electrical conductivity log can be used for discrimination of lithology of unconsolidated sediments in a non-saline pore-water environment, since silts and sands often have different electrical properties. However, in the Fraser delta area, the conductivity log appears to respond primarily to pore-water salinity variations.

The conductivity sonde used for logging all GSC boreholes in the Fraser delta is an inductive tool (Geonics EM-39C) which does not require direct electrical contact with the formation or fluid in the borehole and is relatively insensitive to near-sonde borehole conditions. A detailed description of the sonde and applications is given by Taylor et al. (1989). The sonde configuration results in a measured response of the formation conductivity integrated out to 1 or more meters radially from the borehole and vertical resolution is on the order of 0.5 meters or greater (see Taylor et al.(1989) for a detailed discussion of thin layer response). Unlike the gamma sonde, the time constant of this tool is relatively small; hence a logging speed of 5cm/s or less was used for all surveys, yielding a vertical depth-shift error in conductivity readings less than 5 cm. Sonde calibration was conducted routinely at all borehole locations in the survey area in order to maintain zero offset errors less than +/- 0.1 milliSiemens/meter.

The Holocene delta has been interpreted to have been formed, and distal sediments deposited, in a marine environment (Clague et al., 1991); hence the original pore-water salinity at time of deposition is thought to have been similar to seawater. The present day salinity of the Holocene sediments has been interpreted to represent the response to groundwater flow governed by aquifers and aquitards within both Holocene and Pleistocene sediments (Ricketts, 1998). Saline pore-water is common throughout the vertical Holocene section associated with fine-grained silts and clays, and saline conditions may extend to depths of 300 meters or more (Dallimore et al., 1995; Dallimore et al., 1996). Fresh-water zones do occur near surface, within the Holocene section; the thicknesses of these zones may vary between 1 meter and 40 meters, and are often (but not always) associated with sand units. An inverse conductivity gradient (decreasing ) with depth is almost always associated with the basal portions of the lower (fine-grained) Holocene distal deltaic sediments, and commonly a low conductivity (non-saline pore-water) condition exists at the Holocene-Pleistocene boundary. Examples of electrical conductivity logs with such gradients are compared in the report on the Mud Bay well (in this open file).

Such gradients can occur over vertical distances between 2 meters and 70 meters.. Since the basal Holocene fine-grained unit is considered to be an aquitard (Ricketts, loc.cit.) with very low permeability, it is suggested that the pore-water salinity in these basal silts may have been altered since deposition and may reflect a significant groundwater head as well as horizontal flow within aquifers below the Holocene-Pleistocene boundary.

The measured electrical conductivity response of unconsolidated earth materials is a function of the pore-water conductivity, porosity, degree of porewater saturation and grain surface conductivity; this relationship has been developed from an empirical relationship originally give by Archie (1942), and the current form of it, as used in groundwater studies (after Frohlich and Parke , 1989) is as follows:

$$C_{obs} = C_{wat} * (F_m/a) * S_n + C_g \quad (1)$$

where:

Cobs = observed formation conductivity (milliSiemens/m)

Cwat= porewater conductivity (milliSiemens/m)

F = formation porosity (fractional)

m = the "cementation factor" (dimensionless constant)

a = the "grain geometry factor" (dimensionless constant)

S = pore saturation (fractional)

n = the "saturation exponent" (dimensionless)

Cg = the "grain surface" conductivity (milliSiemens/m)

In porous formations with high pore-water salinity, most of the formation electrical conductivity response is due to the pore-water electrical conductivity and the "grain surface" conductivity can be assumed to be negligible (Frohlich and Parke, loc. cit.). However, the salinity-conductivity relationships for seawater solutions (assumed to be the pore-water within the Holocene deltaic sediments of the Fraser delta) is temperature-dependent (Popov et al., 1979; Dera, 1992) even over the limited temperature ranges observed in deep boreholes (Dallimore et al., 1995). Hence to obtain the "cementation" m, and "grain geometry" a, constants for Fraser delta sediments from equation (1), one would require accurate measurements of formation conductivity, porewater salinity, formation temperature, porosity and porewater saturation over a wide range of values. As yet, there is insufficient data for such as statistical fit to equation (1); however, such studies are currently on-going as more detailed geotechnical and geophysical borehole data becomes available (Dallimore et al., 1995; Dallimore et al. 1996).

From detailed deep drilling and geotechnical sampling given by Dallimore et al. (1995), a direct empirical relationship between pore-water salinity and formation electrical conductivity has been attempted for combined measurements of Holocene and Pleistocene sediments of the Fraser delta. The data base (from GSC boreholes FD94-3, FD94-4, FD95-S1, and FD96-1) and the linear relationship is given by Hyde and Hunter (1998). The derived relationship is as follows:

$$SL = [(C_{obs} - 15.26) / 35.7] 1.12 \pm 2.2 \text{ (95\% conf. lim.)} \quad (2)$$

where:

SL = pore water salinity (g/l)

Cobs= formation electrical conductivity (milliSiemens/m)

Since the relationship given in equation (2) was derived from a variety of sediment types over a relatively narrow fractional porosity range between .4 and .5, the statistical error tends to confirm the overriding contribution to the formation conductivity as that of pore-water salinity, and those of temperature and grain conductivity are small. Assuming the above porosity range to be representative for unconsolidated sediments in the Fraser delta, this relationship can be used to estimate variations of pore-water salinity in other places within the survey area where borehole and surface electrical conductivity measurements are made; an example of such an

application is given by Christian et al. (1998).

### The Magnetic Susceptibility Log

The magnetic susceptibility of earth materials represents the degree to which they can be magnetized in the presence of the earth's magnetic field and is defined as the ratio of the intensity of magnetization divided by the magnetic field strength (Telford et al., 1976). Large magnetic susceptibility responses are associated with ferrimagnetic minerals, such as those composed of iron-titanium oxides; of these, magnetite exhibits by far the highest susceptibility values (Lindsley et al., 1966). Often however, unconsolidated sediments, such as those in the Fraser delta, contain only small quantities of ferrimagnetic minerals; hence the overall magnetic susceptibility responses are, in general, low compared to igneous rocks and many metamorphic and sedimentary rocks. It is most probable that the magnetic susceptibility response in fluvial deltaic, as well as glacially-derived sediments reflect only the magnetite content of the material (McNeil et al, 1996).

The magnetic susceptibility borehole logging sonde used in the study area (Geonics Em-39M) was designed and tested by means of a joint GSC-industry co-operative research initiative. It was initially considered as an experimental prototype, but has subsequently become a commercial product. Initial results from the Fraser delta are given by Hunter et al. (1995) and more widespread testing results are given by McNeil et al., (1996). The sonde is based on an electromagnetic inductive design similar to the electrical conductivity sonde (Geonics EM-39C) and the digital recording configuration (as well as logging speed parameters) are similar. Although the tool is relatively insensitive to near-sonde borehole conditions, the penetration into the formation is somewhat less than the conductivity sonde (approximately 30 cm response radius). Detailed discussions of the theory of operation as well as resolution are given by McNeil et al. (1996). For applications in boreholes within the Fraser delta, calibration of the tool was routinely done to a resolution of  $\pm 0.01 \times 10^{-3}$  S.I.

Example magnetic susceptibility logs showing large contrasts can be seen in boreholes FD95-S1 and FD94-4 as well as in most other boreholes where the Holocene-Pleistocene boundary has been encountered. Within the Holocene sediments of the study area, the magnetic susceptibility (hence magnetite content) of the sediments is quite low; there are however, slight variations in response between fine grained (low) and coarse grained (high) sediments. In contrast, the Pleistocene sediments appear in general to contain relatively much higher magnetite content, and the Holocene-Pleistocene boundary is usually marked by a large magnetic susceptibility contrast.